Research Square

Preprints are preliminary reports that have not undergone peer review.
They should not be considered conclusive, used to inform clinical practice,
or referenced by the media as validated information.

Gyre dynamics modulate northward throughput of Gulf Stream water to subpolar latitudes

Helene Asbjørnsen

H.Asbjornsen@uib.no

University of Bergen https://orcid.org/0000-0002-2959-3482

Lea Svendsen

University of Bergen https://orcid.org/0000-0002-0181-3332

Yanchun He

Nansen Environmental and Remote Sensing Center, Bjerknes Centre for Climate Research
https://orcid.org/0000-0002-5932-3627

Tillys Petit

National Oceanography Centre https://orcid.org/0000-0002-7922-9363

Article

Keywords:

Posted Date: June 4th, 2026

DOI: https://doi.org/10.21203/rs.3.rs-9910336/v1

License: This work is licensed under a Creative Commons Attribution 4.0 International License.
Read Full License

Additional Declarations: There is **NO** Competing Interest.

Gyre dynamics modulate northward throughput of Gulf Stream water to subpolar latitudes

Helene Asbjørnsen[1,2*], Lea Svendsen[1,2], Yanchun He[3,2], Tillys Petit[4]

[1*]Geophysical Institute, University of Bergen, Bergen, Norway.
[2]Bjerknes Centre for Climate Research, Bergen, Norway.
[3]Nansen Environmental and Remote Sensing Center, Bergen, Norway.
[4]National Oceanography Centre, Southampton, UK.

*Corresponding author(s). E-mail(s): h.asbjornsen@uib.no;
Contributing authors: lea.svendsen@uib.no; yanchun.he@nersc.no; tillys.petit@noc.ac.uk;

Abstract

The northeastward transport of Gulf Stream water is a major conduit for heat in the Atlantic Ocean, shaping climate across the Arctic-Atlantic region. Variability in the amount of Gulf Stream water that is 'throughput' to subpolar latitudes gives rise to a potential for predicting temperatures further north, but is not well understood. Here, we use Lagrangian techniques to quantify the throughput of Gulf Stream water in an eddy-rich ocean model. We find distinct interannual variability related to the strength of the wind field. During transitions to negative North Atlantic Oscillation (NAO) conditions, the tilt of subsurface density-surfaces reduce due to weakened vertical Ekman velocities in the gyres. This reduces the baroclinicity of the North Atlantic Current and results in increased subsurface throughput of Gulf Stream water. The results demonstrate how gyre dynamics impact the upper-branch of the Atlantic Meridional Overturning Circulation (AMOC) by modulating the northward throughput of Gulf Stream water.

1 Introduction

The Gulf Stream and its northward extensions are important currents in the Atlantic Ocean, carrying warm and saline water from subtropical to subpolar latitudes. Although changes in ocean circulation has been shown to impact European climate on time scales ranging from interannual (e.g., Duchez et al. 2016) to multidecadal (e.g., Sutton and Dong 2012; Årthun et al. 2018), fundamental questions about key components of the ocean circulation remain unanswered. For instance, it is unknown to what extent gyre dynamics impact the northward 'throughput' of water from the subtropical gyre to the subpolar gyre, and consequently influence the upper limb of the Atlantic Meridional Overturning Circulation (AMOC).

In monitoring the AMOC at subtropical and subpolar latitudes, measurements from the RAPID (Smeed et al. 2026) and OSNAP (Fu et al. 2025) arrays indicate that there is limited meridional coherence

in the AMOC on interannual time scales, consistent with results from coarse resolution climate models (Bingham et al. 2007; Zhang 2010; Gu et al. 2020). Similarly, upper-ocean components in the extended Gulf Stream system show little meridional coherence across the gyre structures on interannual to decadal time scales (Asbjørnsen et al. 2024). This poses a major challenge when looking for early warning signs of a potential basin-wide AMOC slowdown on longer time scales as a consequence of global warming (Frajka-Williams et al. 2023; Petit et al. 2025). Obtaining a better understanding of the variability in the amount of Gulf Stream water recirculating locally in the subtropical gyre versus the amount transported northeastward in the North Atlantic Current is therefore important for assessing the connection between subtropical and subpolar latitudes.

Lagrangian methods is a powerful tool for investigating exchanges across the North Atlantic gyre structures, with past approaches ranging from tracking surface drifters (Brambilla and Talley 2006; Rypina et al. 2011) to profiling floats (Kwon and Riser 2005) and virtual water particles in ocean models (Burkholder and Lozier 2011; Desbruyères et al. 2013; Foukal and Lozier 2016; Berglund et al. 2022; Tooth et al. 2024). These studies have revealed that the main connection between subtropical and subpolar latitudes occurs in subsurface layers, with water flowing northeastward along sloping isopycnals following densification within the subtropical gyre. It does, however, remain unclear which mechanisms drive enhanced northward throughput from the subtropical gyre to the subpolar gyre. With an emphasis on decadal surface intrusions of subtropical water, Häkkinen et al. (2011) showed that weakened climatological wind stress curl is linked to periods of enhanced surface intrusions when density surfaces relax, the subpolar front moves west, and subtropical water outcrops in the eastern subpolar gyre. However, this mechanism does not in itself explain volume transport variability of Gulf Stream water at depth where the majority of the transport occurs.

Here, we seek to 1) quantify variability in the northward throughput from the subtropical gyre to the subpolar gyre, and 2) provide a dynamically consistent mechanism explaining variability in the subtropical-subpolar throughput on interannual time scales. We thus focus on the part of the circulation that connects the subtropical gyre to the subpolar gyre in the upper-ocean through northeastward transport in the North Atlantic Current. Using a volume conserving Lagrangian trajectory model, we construct volume transport times series of the subtropical recirculation and the subtropical-subpolar throughput based on an eddy-rich ocean hindcast. We find that wind-driven Ekman dynamics in the gyres are an important modulator of the subtropical-subpolar throughput through changing the slope of subsurface isopycnals and with that the baroclinicity of the North Atlantic Current.

2 Methods

2.1 Ocean hindcast simulation

To quantify the recirculation within the subtropical gyre versus the throughput to the subpolar gyre, we use the simulated velocity field in the GO8p7-eORCA12 ocean-sea ice hindcast (Megann et al. 2022; Marsh et al. 2024). The GO8p7-eORCA12 hindcast is based on the NEMO version 4.0.4 ocean model (Madec et al. 2019) coupled to the CICE sea ice model (Hunke et al. 2017) and forced by the JRA-55 atmospheric reanalysis (Tsujino et al. 2018). The hindcast is initialized from rest in 1958 with mean 1995-2014 temperature and salinity from the EN4 product (Good et al. 2013). The configuration uses the eORCA12 grid with a 1/12° horizontal resolution, and is thus considered eddy-rich. The GO8p7-eORCA12 grid has 75 vertical levels with a nonlinear free surface where the variation of column thickness due to surface variation is distributed over the full water column for improved flow over steep topography (Adcroft and Campin 2004). Vertical mixing is parameterized using an updated version of the Turbulent Kinetic Energy scheme (Gaspar et al. 1990; Madec et al. 2019).

Here, we focus on interannual variability in the ocean circulation over the last three decades of the GO8p7-eORCA12 hindcast starting our analysis in 1990. This minimizes the effect of model spin-up on our results. Subtropical AMOC variability is represented well in the hindcast compared to observations at 26.5°N at the RAPID line (Figure S1a), with a somewhat weaker mean strength than in observations (15.5 Sv in the hindcast versus 17.1 Sv in observations for the 2004-2021 period, respectively) related to a 4 Sv weaker Florida Current volume transport compared to the Florida Straits cable measurements (Figure S1b). The GO8p7-eORCA12 hindcast has also been shown to represent well subpolar AMOC variability at the OSNAP line, with a slightly weaker net northward transport compared to observations (Tooth et al. 2025).

2.2 Lagrangian tracking with TRACMASS

The Lagrangian analysis tool TRACMASS is used to evaluate the advective pathways and transports of the Gulf Stream water. The TRACMASS algorithm (here version 7.1; Aldama-Campino et al. (2020) is based on the continuity equation of mass, computing the trajectory paths analytically from the volume transports at the model grid cell faces (Döös 1995). We use the 1990-2021 monthly mean zonal and meridional velocities from the GO8p7-eORCA12 hindcast and apply the piece-wise stationary scheme with 120 intermediate time steps per month over which velocities are linearly interpolated in time. The vertical velocities are computed from the continuity equation to guarantee mass conservation within the TRACMASS framework (Döös et al. 2017).

For the Lagrangian experiment we seed particles in the Gulf Stream at 30°N (Figure 1a). At this latitude the Gulf Stream flows as a single core following the shelf break as seen in Figure S2. The flow

across the seeding section thus has a simpler structure than at, for instance, 26.5°N where the Florida Current and the Antilles Current flow as two separate branches with their own variability (Meinen et al. 2019). The Lagrangian particles are seeded at monthly resolution during 1990-2017 and tracked forward in time for four years. The seeding is scaled with the time-varying Gulf Stream volume transport with each particle representing maximum 0.005 Sv, sufficient to achieve robust Lagrangian statistics for each seeding time step (e.g., Jones et al. 2016). With a monthly mean Gulf Stream transport of around 40 Sv, about 2.7 million particles are tracked in total for the 1990-2017 seeding period.

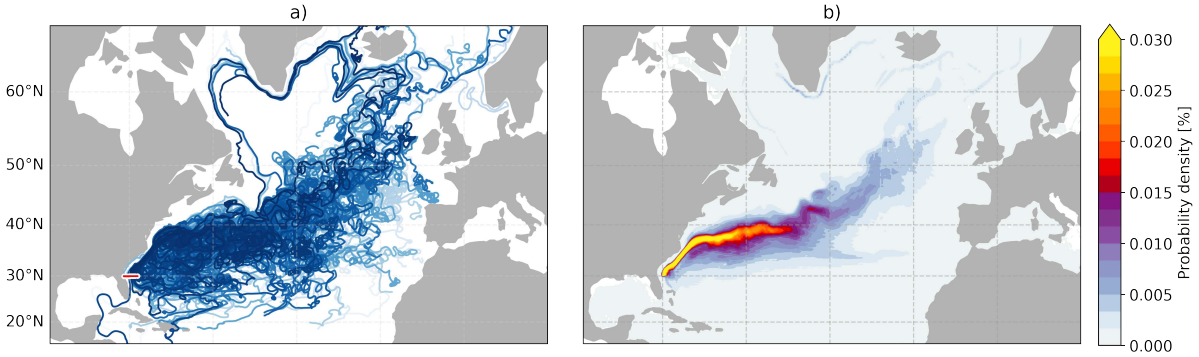


Fig. 1 Pathways of Gulf Stream water. (a) Trajectories of 200 randomly selected particles seeded in January 2017 and tracked for four years. The individual particle trajectories are shown in different shades of blue. The seeding section at 30°N is shown in red. (b) Particle probability density binned at 1/4° resolution based on all particles seeded during 1990-2017 and tracked forward in time for four years. The probabilities have been weighted by the volume transport represented by the particles. The displayed probabilities sum to 100%.

2.3 Particle probability density and significance tests

To visualize the large-scale advective pathways of the Gulf Stream water, we bin all particle positions over the four years of tracking into a histogram weighted with the particle volume transport. This gives us the volume transport weighted probability density as expressed by:

$$P_{i,j} = \frac{w_{i,j} N_{i,j}}{\sum wN} \times 100\% \tag{1}$$

where $P_{(i,j)}$ is the probability density in the bin index i,j. $N_{(i,j)}$ is the number of particles that has been present in the bin during the four years of tracking and w is the weighting by the volume transport attached to those particles. $\sum wN$ is the sum of all volume transport weighted particle counts for all bins. We choose a bin of $1/4° \times 1/4°$, which is coarser than the ocean model grid, to highlight large-scale circulation features (Figure 1b).

All correlations stated throughout are the Pearson correlation coefficient r and have p-levels smaller than 0.05 (significance at the 95% confidence level). For the regression analysis between the time series of throughput variability and different spatiotemporal variables linked to large-scale circulation patterns

(Section 3.2), significance at the 90% confidence level is indicated in hatching in the respective figures using a two-sided Wald test with t-distribution.

3 Results

3.1 Quantification of throughput and recirculation

In tracking the Gulf Stream water, we identify three main pathways: immediate subtropical recirculation, basin-wide subtropical recirculation, and the North Atlantic Current (Figure 1). The immediate subtropical recirculation tends to occur shortly after the Gulf Stream separates from the coast at 35°N (Hogg 1992), and water following this pathway will either continue circulating in the interior of the subtropical gyre or rejoin the western boundary current further south. The basin-wide recirculation follows the Azores Current eastward and recirculate south over a range of longitudes with the Canary Current as its easternmost branch (e.g., Pérez-Hernández et al. 2023). The North Atlantic Current transports water northeastward, and is the main pathway of interest in terms of throughput to the subpolar gyre.

The North Atlantic Current is known to flow past the Grand Banks and cross the Mid-Atlantic Ridge as three main branches in the vicinity of the Maxwell Fracture Zone, Faraday Fracture Zone, and Charlie–Gibbs Fracture Zone located between 48°N and 53°N (Daniault et al. 2016). Similarly, Figure 1 shows a wide range of trajectory paths reaching subpolar latitudes, with the northernmost trajectories passing through the Northwest Corner before veering sharply east and the southernmost trajectories being more likely to recirculate south along the European continental shelf after reaching subpolar latitudes.

We quantify the northward throughput to the subpolar gyre versus the subtropical recirculation using a simple geographical criterion (Figure 2). The volume transport represented by particles crossing 45°N within the four years of tracking is considered as the throughput, while volume transport represented by particles not crossing 45°N is considered as recirculation. As seen in Figure 2c, the typical transit time to 45°N is between three months and two years. It is therefore sufficient to track the particles for four years. The interannual variability in throughput is not particularly sensitive to the exact geographical criteria used. For instance, the throughput volume transport using a 50°N criterion correlates at $r = 0.89$ to using the 45°N criterion. We do note that some particles recirculate back south after crossing 45°N (around 4 Sv after four years of tracking), but we choose to keep these in the throughput group as they follow the North Atlantic Current north prior to returning south.

Our results show an average recirculation of 24.5 ± 2.1 Sv and a throughput of 14.2 ± 1.3 Sv. This equates to 63% and 37% of the mean Gulf Stream transport of 38.7 ± 2.0 Sv, respectively. The majority of the water being recirculated is expected as the Gulf Stream transport at 30°N is considerably higher than observational estimates of subtropical water in the North Atlantic Current. Roessler et al. (2015) estimate that the North Atlantic Current transports an average of 27.0 Sv, of which 60% (16.2 Sv) is

subtropical water and the remaining 40% (10.8 Sv) is subpolar water. The throughput of 14.2 Sv of subtropical water found here is consistent with the observational estimate considering that the mean circulation in the hindcast is slightly weaker than in observations (Figure S1).

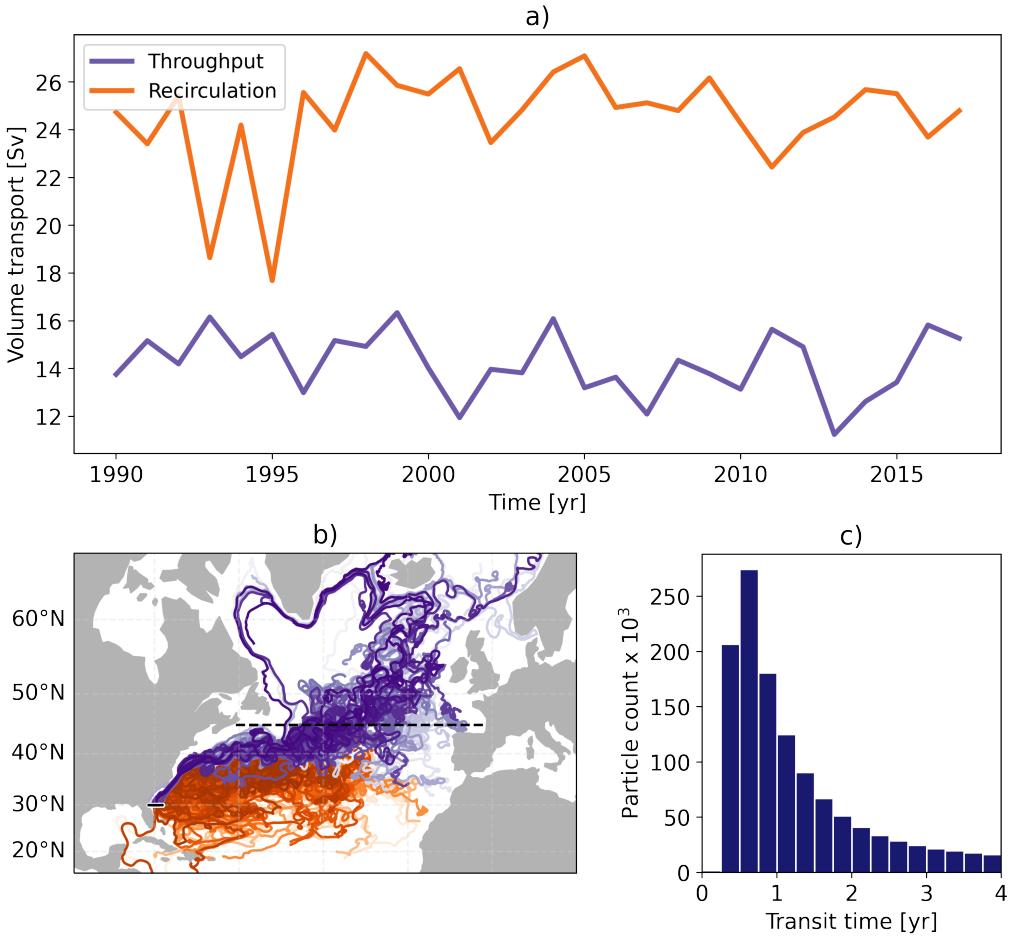


Fig. 2 Quantification of recirculation versus throughput. (a) Annual mean volume transport time series of the northward throughput to the subpolar gyre (purple) and the recirculation within the subtropical gyre (orange). The time on the x-axis represents the seeding time at 30°N. The two time series sum to the net Gulf Stream transport at 30°N. (b) The same trajectories as in Figure 1a, but with recirculation marked in shades of orange and throughput marked in shades of purple. The 45°N quantification criterium is marked with a black dashed line. (c) Histogram showing the transit time to 45°N from the seeding section at 30°N for all particles reaching 45°N within four years of tracking. The 90th percentile is at 2.45 years.

Both the recirculation and the throughput time series in Figure 2a display distinct interannual variability. The recirculation is strongly correlated to the net Gulf Stream transport at the seeding section ($r = 0.79$). The close relationship is to be expected as the Gulf Stream constitutes the western boundary of the subtropical gyre in addition to compensating for the Deep Western Boundary Current flowing southward at depth (e.g., Asbjørnsen and Årthun 2023). The throughput time series is not significantly correlated to the net Gulf Stream transport, but is weakly anticorrelated to the recirculation ($r = -0.40$) suggesting that a strong northward throughput tends to coincide with weaker gyre recirculation. The variability quantified in the time series is reflected in the pathways of the water as seen in the probability density anomaly from the mean (Figure 3a-b, Figure S3). For instance, particles seeded in 1995 show

less water being recirculated in the subtropical gyre, with a larger fraction than in climatology being transported north in the North Atlantic Current (Figure 3a). Following the 2013 seeding, distinctly less water is throughput to the subpolar gyre with more water than in climatology recirculating with the Azores Current (Figure 3b). These two anomalous years are moreover seen in Figure 2a with a record low recirculation for the 1995 seeding and a record low throughput for the 2013 seeding, confirming that our quantification captures meaningful changes in the circulation.

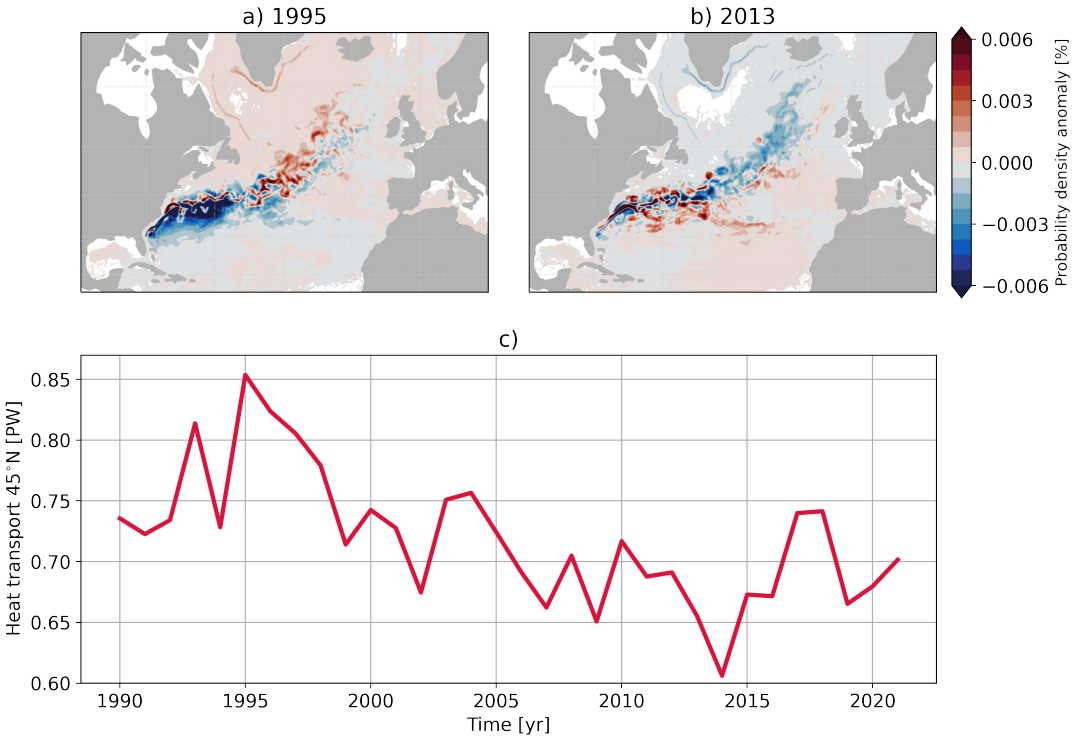


Fig. 3 Shifts in pathways of Gulf Stream water and link to ocean heat transport across 45°N. (a-b) Anomaly from the mean volume weighted probability density distribution (seen in Figure 1b) for particles seeded in (a) 1995 and (b) 2013, respectively. (c) Net northward ocean heat transport across 45°N calculated from the Eulerian temperature and meridional velocity fields (1990-2021). The velocity field has been mass-compensated to ensure that the heat transport is unaffected by choice of reference temperature. The heat transport at 45°N correlates with the throughput time series (Figure 2a; purple line) at zero lag ($r = 0.40$) and at one-year time lag ($r = 0.40$), significant at the 95% confidence level.

We find a significant relationship between variability in the throughput volume transport and the ocean heat transport into the subpolar North Atlantic (Figure 3c). The heat transport at 45°N correlates with the throughput time series (sorted by seeding time) at zero lag ($r = 0.40$) and with a one-year time lag ($r = 0.40$). This implies that 16% of the interannual variability in heat transport across 45°N can be explained by variability in the subtropical-subpolar throughput. While 16% is a considerable fraction, it likely reflects some temporal 'smearing' due to the range in transit times from the seeding section (Figure 2c). It also indicates that other processes are important for the heat transport across 45°N. For instance, we expect variability in the temperature of the source water and along-path watermass modification from surface heat loss and mixing with subpolar waters to play a role (e.g., Asbjørnsen et al. 2021; Stevens et al. 2020). Additionally, changes in the deep ocean circulation will affect the net ocean heat transport

across 45°N (Biló et al. 2024; Koman et al. 2024). However, the significant relationship between the subtropical-subpolar throughput and the net heat transport at 45°N indicates that understanding the mechanisms driving variability in the throughput would help predicting major changes in subpolar heat content. We note, for instance, that the record low throughput following the seeding in 2013 is consistent with anomalously low heat transport across 45°N in 2014, leading up to the widely reported subpolar cold-blob in 2015 (e.g., Duchez et al. 2016; Sanders et al. 2022).

3.2 Mechanisms of throughput variability

Since there is no statistically significant relationship between the subtropical-subpolar throughput and variability in the net Gulf Stream transport, we seek to determine under which conditions the throughput from the subtropical gyre to the subpolar gyre is enhanced. Focusing on interannual time scales, we explore spatial atmospheric circulation variables such as sea level pressure and wind stress curl as well as variables related to ocean circulation such as the vertical Ekman velocity, large-scale density field, sea surface height, and the barotropic streamfunction. By regressing the different spatial fields onto the throughput time series, we identify the large-scale circulation patterns most closely associated with variability in the subtropical-subpolar throughput.

The regression patterns in Figure 4 show the typical sea level pressure anomalies associated with a strengthened subtropical-subpolar throughput. Because the throughput time series is sorted by the seeding year and the most common transit time to 45°N is between three months and two years, we show the regressions at zero lag, one-year lag, and two-year lag with the sea level pressure lagging the seeding year. The sea level pressure anomalies show a transition from relatively strong atmospheric circulation at lag year zero (Figure 4a) to a weakening of the Icelandic Low at lag year one, with development of a weak Azores High at lag year two (Figure 4b-c). Comparing the regression patterns in Figure 4 to the EOF-derived NAO spatial pattern (as in e.g., Hurrell and Deser (2010)) gives spatial correlations of $r = 0.75$ (Figure 4a; resembles NAO^{+}), $r = -0.32$ (Figure 4b), and $r = -0.83$ (Figure 4c; resembles NAO^{-}), respectively. We do, however, note that for instance the Azores High anomaly in Figure 4c is shifted northeast of the canonical NAO^{-} loading pattern. The weakened sea level pressure compared to climatology is associated with weakened wind stress curl (Figure S5e), particularly over the Irminger Sea which is a region of strong climatological positive wind stress curl (Figure S4e). The regression patterns in Figure 4 are robust to removing single years from the analysis, for instance at the edge years (1990, 2017) or extreme years (1995, 2013).

To investigate whether the anomalous atmospheric circulation seen in Figure 4 impacts vertical motion in the gyres, we derive the vertical Ekman velocity from the wind stress curl and regress it onto the throughput time series (Figure 5a,c,e). In climatology, the interior of the subtropical gyre is associated with net Ekman pumping (downward motion), while the subpolar gyre is associated with net Ekman

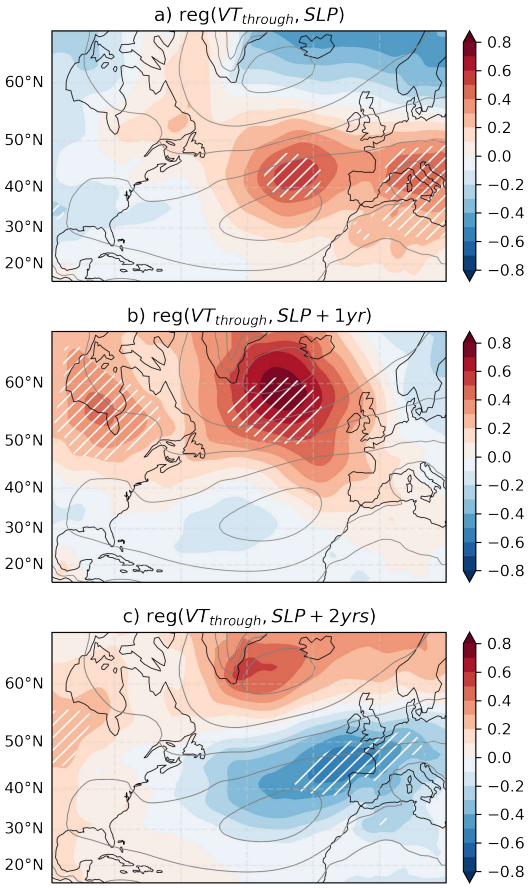


Fig. 4 Throughput variability and large-scale patterns in sea level pressure. Annual mean sea level pressure ('SLP', hPa) regressed onto the annual mean throughput time series ('through'; Sv). Because the throughput time series is sorted by the seeding year at 30°N and the particles typically use between three months to two years to reach 45°N, we show the regression at zero lag time (a), SLP lagging with one year (b), and SLP lagging with two years (c). The throughput time series has been standardized and the unit is hPa per standard deviation of volume transport. Significance at the 90% confidence level is indicated in hatching. Climatological sea level pressure (1990-2021) is show in grey contour lines (contour levels; 1005:4:1021 hPa).

suction (upward motion) (Figure S4f). The vertical Ekman velocity pattern associated with strengthened throughput shows weakened upward motion in the subpolar gyre (Figure 5c) and a weakened downward motion in the northeast of the subtropical gyre (Figure 5e). These anomalies in the vertical Ekman velocity is likely to have an impact on isopycnal depths in both the subtropics and in the subpolar North Atlantic.

Next we explore the associated potential density anomalies at 100 m depth, which is near the base of the Ekman layer (Rio and Hernandez 2003). The potential density anomaly patterns show that enhanced throughput is associated with increased densities in the subtropical region and decreased densities in the subpolar region at lag year one and two after particle seeding in the Gulf Stream (Figure 5d,f). This pattern indicates reduced meridional density gradients and a relaxation of subsurface isopycnals (generally sloping upwards from southwest to northeast) consistent with reduced vertical motion in the respective gyres. The same signal is seen in the layers above 100 m depth but gets weaker in the layers below 100 m depth (not shown). The density anomaly patterns shown in Figure 5 are moreover reproduced when regressing the potential density derived from the gridded observational product EN4.2.2 (Good

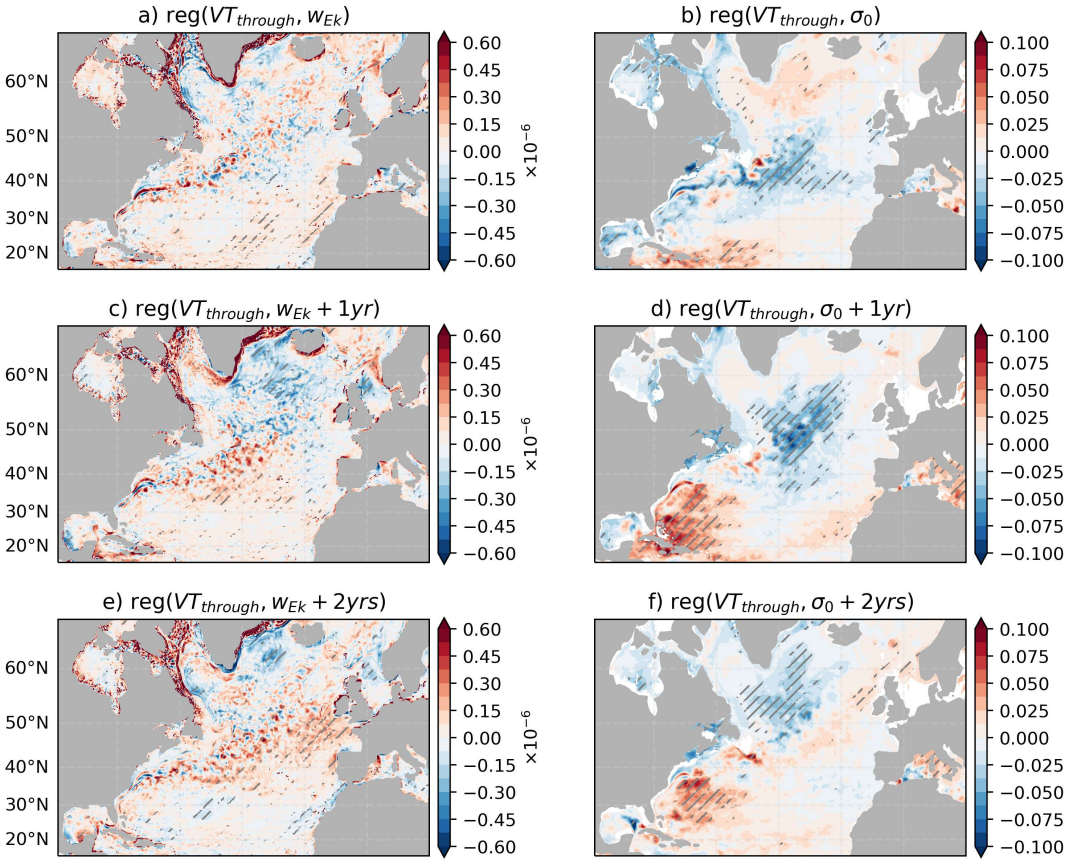


Fig. 5 Throughput variability and large-scale patterns in subsurface densities and vertical Ekman velocity. (a,c,e) Annual mean vertical Ekman velocity derived from wind stress curl ('w_{Ek}', m/s) regressed onto the annual mean throughput time series ('through'; Sv). The throughput time series has been standardized and the unit is m/s per standard deviation of volume transport. (b,d,f) Annual mean potential density at 100m depth ('σ_0'; kg/m^3) regressed onto the annual mean throughput time series ('through'; Sv). The throughput time series has been standardized and the unit is kg/m^3 per standard deviation of volume transport. (a-f) Significance at the 90% confidence level is indicated in hatching.

et al. 2013) onto the throughput time series from the Lagrangian experiment (Figure S6). The EN4.2.2 data is independent from the GO8p7-eORCA12 hindcast apart from the model initialization, and thus links the density variability in the model simulation to observed variability. Notably, the 100 m density anomalies are not entirely co-located with the vertical Ekman velocity anomalies, but this is somewhat expected as there will be ocean adjustments from advection and wave propagation within the averaging period when using annual mean fields. There might also be other drivers of density anomalies at 100 m depth than wind-induced vertical velocities, such as horizontal advection and surface heat fluxes. For instance, colder subtropical and warmer subpolar regions are characteristic for NAO$^-$ conditions (e.g., Wanner et al. 2001), and will give density anomalies of the same sign that Figure 5d,f show.

Because ocean current velocities are more directly governed by pressure-gradients than by density-gradients alone, we calculate the meridional gradient in the thickness of the layer with densities lighter than $\sigma_0 = 26.5$ (i.e. the $\sigma_0 < 26.5$ potential density layer). The thickness layer gradient (ΔZ) is calculated as the difference between the zonal mean layer thickness at a subpolar latitude (50°N) and a subtropical latitude (30°N). The average layer thickness is roughly 50 m at 50°N and 350 m at 30°N (Figure S7). The time-evolving difference represents the subtropical-subpolar gradient in the layer thickness marked

by the $\sigma_0 < 26.5$ isopycnal (Figure 6). We find that a reduced layer thickness gradient between subpolar and subtropical latitudes is linked to higher northward throughput of subtropical water ($r = 0.63$ at a 1-year time lag with the thickness gradient lagging because the throughput is sorted by seeding time). The relationship between subtropical-subpolar throughput and the layer thickness gradient appears particularly strong for the extreme years such as the record high throughput that follows the 1999 seeding and record low throughput that follows the 2013 seeding. Analysis of sea surface height does not reveal meridional gradients that could explain the changes in the thickness layer gradient (Figure S5d,g). We therefore mainly connect the changes in the thickness of the $\sigma_0 < 26.5$ layer to vertical movement of the 26.5 isopycnal. While baroclinic changes in the North Atlantic Current through changes in the density gradients seem to dominate variability in subtropical-subpolar throughput, we note that locally elevated sea surface height in the Gulf Stream (Figure S5a) and the North Atlantic Current (Figure S5d) tends to be associated with higher throughput of warm subtropical water, consistent with thermal expansion effects.

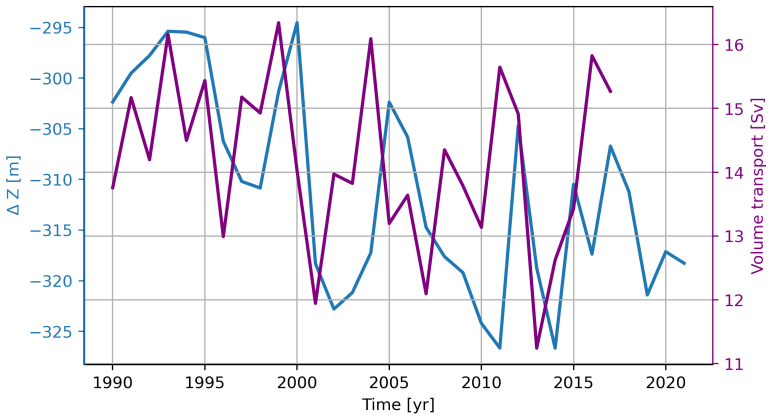


Fig. 6 Layer thickness gradient and throughput variability. Left axis; Difference between the zonal mean thickness of the $\sigma_0 < 26.5$ layer at 50°N and at 30°N ('ΔZ'; blue line), where σ_0 is the potential density. Right axis; Throughput volume transport time series sorted by seeding time (purple line). The time series are significantly correlated at a 1-year lag ($r = 0.63$) with a smaller thickness difference related to a higher throughput. The 1-year lag results from the throughput time series being sorted by seeding time and spending three months to two years reaching subpolar latitudes.

Previous Lagrangian studies have established that the throughput of water from the subtropics to subpolar latitudes mainly occurs in subsurface layers (e.g., Burkholder and Lozier 2011; Foukal and Lozier 2016; Asbjørnsen et al. 2021). Whether interannual variability is also dominated by the subsurface layers below the Ekman layer is key for understanding the dynamics of the throughput variability. Figure 7 shows the throughput time series sorted by seeding year as in Figure 2a, but with the depth classes at the seeding time versus the depth classes when crossing 45°N. The highest volume transport occurs in the 100-200 m and 200-300 m depth classes. There is somewhat of a shoaling in the transport depths from seeding (Figure 7a) to the transport depths when crossing 45°N (Figure 7b). For instance, transport in the 50-100 m depth class increases from approximately 1 Sv at seeding to 2 Sv at crossing 45°N. At the time of crossing 45°N, the 50-100 m, 100-200 m, and 200-300 m depth layer transports are strongly

correlated to the net throughput ($r = 0.86$, $r = 0.89$, $r = 0.86$, respectively). This finding points to a mechanism where subsurface transports strengthen when large-scale atmospheric circulation weakens and subsurface isopycnals relax compared to climatology.

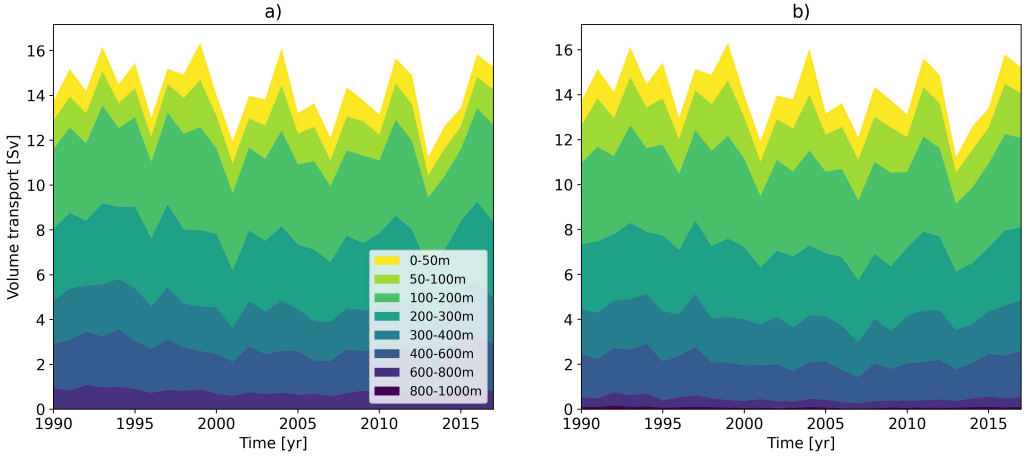


Fig. 7 Depth classes of the subtropical-supolar throughput. (a) Throughput volume transport sorted by seeding time binned into depth classes at seeding. (b) Throughput volume transport sorted by seeding time binned into depth classes when crossing 45°N.

Based on our results, we propose a new mechanism explaining variability in the subtropical-subpolar throughput on interannual time scales (Figure 8). As shown in the illustration, the subtropical gyre is characterized by Ekman transport convergence, elevated sea surface height, and Ekman pumping (downward motion) pushing subsurface isopycnals down. In contrast, the subpolar gyre is characterized by Ekman transport divergence, depressed sea surface height, and Ekman suction (upward motion) lifting subsurface isopycnals. The isobars and isopycnals are not parallel, meaning that the North Atlantic Current is a baroclinic current intensified at the surface. Based on our results, we propose that as a fast response to weakening in the atmospheric circulation (Figure 4, Figure S5e), Ekman pumping/suction in the subtropical/subolar gyre weakens and isopycnal surfaces relax (Figure 8b). This reduces the baroclinicity of the North Atlantic Current which allows for enhanced subsurface flow of subtropical water, leading to a strengthening throughput from the subtropical gyre to the subpolar gyre. Similarly, when atmospheric circulation strengthen, Ekman pumping/suction in the subtropical/subpolar gyre strengthens, isopycnal surfaces steepen, baroclinicity increases, and the subsurface transport of subtropical water in the North Atlantic Current is reduced (Figure 8a).

4 Discussion and conclusions

Using Lagrangian techniques, we have quantified the throughput from the subtropical gyre to the subpolar gyre during 1990-2017 in an eddy-rich ocean hindcast. We find distinct interannual variability in the throughput with a standard deviation of 1.3 Sv with implications for poleward ocean heat transport (Figure 2a, Figure 3c). While the ocean adjusts to forcing on a range of timescales (e.g, Johnson and

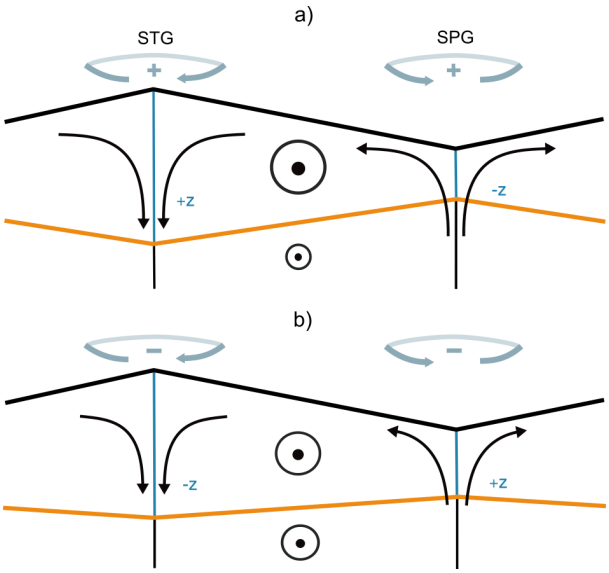


Fig. 8 Mechanism of subtropical-subpolar throughput variability. The idealized schematic shows the subtropical gyre (STG) with Ekman transport convergence and elevated sea surface height and the subpolar gyre (SPG) with Ekman transport divergence and depressed sea surface height. (a) Low throughput. Wind stress curl is strengthened and the Ekman pumping/suction in the subtropical/subpolar gyre is enhanced. Subsurface isopycnals (orange line) are more tilted, and the baroclinicity of the North Atlantic Current (circles indicating flow out of the page) is enhanced. (b) High throughput. Wind stress curl is weakened and Ekman pumping/suction in the subtropical/subpolar gyre is reduced. Subsurface isopycnals are less tilted, and the baroclinicity of the North Atlantic Current is reduced. Subsurface volume transport of subtropical water strengthen.

Marshall 2002; Marshall and Johnson 2013), we here identify a fast response to anomalous atmospheric circulation through changes in the slope of subsurface isopycnals impacting the transport of subtropical water in the North Atlantic Current (Figure 8).

We highlight the importance of gyre dynamics in explaining variability in the subtropical-subpolar throughput similarly to, for instance, Hátún et al. (2005) and Häkkinen et al. (2011). Our results align with Häkkinen et al. (2011) in that reduced wind stress curl favors enhanced northward throughput of subtropical water. However, since we focus on variability in the total northward throughput dominated by transport below the Ekman layer (Figure 7b), our mechanism differ from that in Häkkinen et al. (2011) focusing on near-surface intrusions when the subpolar front shifts westward and more subtropical water outcrop in the eastern subpolar gyre. We find a strong signal in upper-ocean density gradients between the gyre structures, which dynamically will influence the baroclinicity of the North Atlantic Current and favor enhanced subsurface throughput of Gulf Stream water when density gradients are weak. Furthermore, we also see that enhanced throughput is associated with a westward contracted subpolar gyre (Figure S5f) similar to findings in Hátún et al. (2005) and Häkkinen et al. (2011). Whether this contraction of the subpolar gyre is an additional driver of enhanced subtropical-subpolar throughput or the shift merely is a coinciding response to the weakened wind stress curl over the eastern subpolar gyre, is unclear from our analysis.

Observational studies utilizing measurements from the North Atlantic Current suggest that the transport tend to be strong during NAO^+ conditions when wind stress curl is strengthened over the northern subpolar gyre (Roessler et al. 2015; Dotto et al. 2025). This relationship has mainly been connected to

strengthened flow of subpolar water in the North Atlantic Current due to stronger subpolar gyre circulation. It is thus not contradictory to our results showing that transport of subtropical water in the North Atlantic Current is enhanced when wind stress curl is weakened under NAO^--like conditions. However, we note that our throughput time series is not directly correlated with the annual mean or winter mean NAO index itself (station-based or EOF-derived), implying that the persistence and transitions between NAO phases may be important. On longer time scales, model experiments show that persistent NAO^+ forcing leads to elevated surface heat loss in the subpolar gyre and enhanced dense water formation which feeds the Deep Western Boundary Current (Eden and Willebrand 2001; Lohmann et al. 2009; Bhagtani et al. 2025). This ultimately leads to a strengthened subtropical AMOC and increased poleward heat transport as a delayed response to the forcing. It is therefore likely that the mechanisms driving variability in subtropical-subpolar throughput is highly time-scale dependent.

It is well known that the relative amount of subtropical and subpolar water masses determine hydrographic properties in the eastern subpolar gyre (Hátún et al. 2005; Desbruyères et al. 2021). Understanding variability in the throughput from the subtropical gyre to the subpolar gyre therefore has implications for predictability of subpolar temperatures (Borchert et al. 2018; Robson et al. 2018). For instance, we see a lower variance in the throughput time series in the 1990s compared to the later periods (Figure 2a). The 1990s has previously been identified as a period with higher predictive skills of subpolar temperatures (Brune et al. 2018), which could potentially be due to a more steady supply of subtropical water during this period.

The apparent lack of meridional coherence between subtropical and subpolar AMOC variability on interannual time scales has challenged our understanding of the large-scale North Atlantic circulation (Frajka-Williams et al. 2023). While recent studies indicate that a range of mechanisms contribute to limit meridional coherence in the AMOC (e.g, Kostov et al. 2021; Han 2023; Fraser et al. 2025; Petit et al. 2025), we consider it likely that variability in subtropical recirculation versus subtropical-subpolar throughput plays a role in restricting meridional coherence to the gyre structures. To isolate the effect of throughput variability on the large-scale AMOC does, however, require dedicated perturbation experiments and will be pursued in future work.

Supplementary information. The manuscript has a supplementary material file containing Figure S1-S7.

Acknowledgements. This research was funded by the Norwegian Research Council project GYRED (grant 352418), supporting H.A., L.S., Y.H., and T.P. In addition, T.P. was supported by the Natural Environment Research Council Grants RAPID Evolution (grant NE/Y003551/1) and ATLANTiS (grant NE/Y005589/1). We would like to thank Kristofer Döös and Jakob Dörr for useful discussions on Lagrangian tracking.

Data availability. The GO8p7-eORCA12 ocean hindcast is publicly available at https://dx.doi.org/10.5285/399b0f762a004657a411a9ea7203493a (Megann et al. 2022). EN4.2.2 data is available at https://www.metoffice.gov.uk/hadobs/en4/download-en4-2-2.html (Good et al. 2013). The JRA-55 atmospheric reanalysis is available at https://doi.org/10.5065/D60G3H5B (Tsujino et al. 2018). The trajectory data produced will be archived and made publicly available prior to any publication.

Code availability. The TRACMASS v7.0 Lagrangian trajectory code is available in the open source GitHub repository https://github.com/TRACMASS/tracmass (Aldama-Campino et al. 2020).

Author contributions. H.A. defined the overall research problem, carried out the analysis, and led the writing of the manuscript. L.S., Y.H., and T.P. all contributed ideas to the analysis, helped refine the methodology, and contributed to the text.

Competing interests. The authors declare no competing interests.

References

Adcroft A, Campin JM (2004) Rescaled height coordinates for accurate representation of free-surface flows in ocean circulation models. Ocean Modelling 7(3-4):269–284. https://doi.org/10.1016/J.OCEMOD.2003.09.003

Aldama-Campino A, Döös K, Kjellsson J, et al (2020) TRACMASS: Formal release of version 7.0 (Version v7.0-beta). https://doi.org/10.5281/zenodo.4337926

Årthun M, Kolstad EW, Eldevik T, et al (2018) Time Scales and Sources of European Temperature Variability. Geophysical Research Letters 45(8):3597–3604. https://doi.org/10.1002/2018GL077401

Asbjørnsen H, Årthun M (2023) Deconstructing Future AMOC Decline at 26.5°N. Geophysical Research Letters 50(14):e2023GL103515. https://doi.org/10.1029/2023GL103515

Asbjørnsen H, Johnson HL, Årthun M (2021) Variable Nordic Seas inflow linked to shifts in North Atlantic circulation. Journal of Climate 34(17):1–50. https://doi.org/10.1175/JCLI-D-20-0917.1

Asbjørnsen H, Eldevik T, Skrefsrud J, et al (2024) Observed change and the extent of coherence in the Gulf Stream system. Ocean Science 20(3):799–816. https://doi.org/10.5194/os-20-799-2024

Berglund S, Döös K, Groeskamp S, et al (2022) The downward spiralling nature of the North Atlantic Subtropical Gyre. Nature Communications 13(1):2000. https://doi.org/10.1038/s41467-022-29607-8

Bhagtani D, McC. Hogg A, Holmes RM, et al (2025) Asymmetric Response of the North Atlantic Gyres to the North Atlantic Oscillation. Journal of Geophysical Research: Oceans 130(6):e2024JC021997.

https://doi.org/10.1029/2024JC021997

Biló TC, Perez RC, Dong S, et al (2024) Weakening of the Atlantic Meridional Overturning Circulation abyssal limb in the North Atlantic. Nature Geoscience 17(5):419–425. https://doi.org/10.1038/s41561-024-01422-4

Bingham RJ, Hughes CW, Roussenov V, et al (2007) Meridional coherence of the North Atlantic meridional overturning circulation. Geophysical Research Letters 34(23):L23606. https://doi.org/10.1029/2007GL031731

Borchert LF, Müller WA, Baehr J (2018) Atlantic Ocean Heat Transport Influences Interannual-to-Decadal Surface Temperature Predictability in the North Atlantic Region. Journal of Climate 31(17):6763–6782. https://doi.org/10.1175/JCLI-D-17-0734.1

Brambilla E, Talley LD (2006) Surface drifter exchange between the North Atlantic subtropical and subpolar gyres. Journal of Geophysical Research 111(C7):C07026. https://doi.org/10.1029/2005JC003146

Brune S, Düsterhus A, Pohlmann H, et al (2018) Time dependency of the prediction skill for the North Atlantic subpolar gyre in initialized decadal hindcasts. Climate Dynamics 51(5-6):1947–1970. https://doi.org/10.1007/S00382-017-3991-4

Burkholder KC, Lozier MS (2011) Subtropical to subpolar pathways in the North Atlantic: Deductions from Lagrangian trajectories. Journal of Geophysical Research 116(C7):C07017. https://doi.org/10.1029/2010JC006697

Daniault N, Mercier H, Lherminier P, et al (2016) The northern North Atlantic Ocean mean circulation in the early 21st century. Progress in Oceanography 146:142–158. https://doi.org/10.1016/J.POCEAN.2016.06.007

Desbruyères D, Thierry V, Mercier H (2013) Simulated decadal variability of the meridional overturning circulation across the A25-Ovide section. Journal of Geophysical Research: Oceans 118(1):462–475. https://doi.org/10.1029/2012JC008342

Desbruyères D, Chafik L, Maze G (2021) A shift in the ocean circulation has warmed the subpolar North Atlantic Ocean since 2016. Communications Earth & Environment 2(1):48. https://doi.org/10.1038/s43247-021-00120-y

Döös K (1995) Interocean exchange of water masses. Journal of Geophysical Research 100:13499–13514. https://doi.org/10.1029/95JC00337

Döös K, Jönsson B, Kjellsson J (2017) Evaluation of oceanic and atmospheric trajectory schemes in the TRACMASS trajectory model v6.0. Geosci Model Dev 10:1733–1749. https://doi.org/10.5194/gmd-10-1733-2017

Dotto TS, Holliday NP, Fraser N, et al (2025) Dynamics and Temporal Variability of the North Atlantic Current in the Iceland Basin (2014–2022). Journal of Geophysical Research: Oceans 130(6):e2024JC021836. https://doi.org/10.1029/2024JC021836

Duchez A, Frajka-Williams E, Josey SA, et al (2016) Drivers of exceptionally cold North Atlantic Ocean temperatures and their link to the 2015 European heat wave. Environmental Research Letters 11(7):074004. https://doi.org/10.1088/1748-9326/11/7/074004

Eden C, Willebrand J (2001) Mechanism of Interannual to Decadal Variability of the North Atlantic Circulation. Journal of Climate 14(10):2266–2280. https://doi.org/10.1175/1520-0442(2001)014⟨2266:MOITDV⟩2.0.CO;2

Foukal NP, Lozier MS (2016) No inter-gyre pathway for sea-surface temperature anomalies in the North Atlantic. Nature Communications 7:11333. https://doi.org/10.1038/ncomms11333

Frajka-Williams E, Foukal N, Danabasoglu G (2023) Should AMOC observations continue: how and why? Philosophical Transactions of the Royal Society A 381(2262). https://doi.org/10.1098/RSTA.2022.0195

Fraser NJ, Fox AD, Cunningham SA (2025) Impact of Ekman Pumping on the Meridional Coherence of the AMOC. Geophysical Research Letters 52(1):e2024GL108846. https://doi.org/10.1029/2024GL108846

Fu Y, Lozier MS, Bower A, et al (2025) Characterizing the Interannual Variability of North Atlantic Subpolar Overturning. Geophysical Research Letters 52(19). https://doi.org/10.1029/2025GL114672

Gaspar P, Grégoris Y, Lefevre J (1990) A simple eddy kinetic energy model for simulations of the oceanic vertical mixing: Tests at station Papa and long-term upper ocean study site. Journal of Geophysical Research: Oceans 95(C9):16179–16193. https://doi.org/10.1029/jc095ic09p16179

Good SA, Martin MJ, Rayner NA (2013) EN4: Quality controlled ocean temperature and salinity profiles and monthly objective analyses with uncertainty estimates. Journal of Geophysical Research: Oceans 118(12):6704–6716. https://doi.org/10.1002/2013JC009067

Gu S, Liu Z, Wu L (2020) Time Scale Dependence of the Meridional Coherence of the Atlantic Meridional Overturning Circulation. Journal of Geophysical Research: Oceans 125(3):e2019JC015838. https://doi.org/10.1029/2019JC015838

Häkkinen S, Rhines PB, Worthen DL (2011) Warm and saline events embedded in the meridional circulation of the northern North Atlantic. Journal of Geophysical Research 116(C3). https://doi.org/10.1029/2010JC006275

Han L (2023) Exploring the AMOC Connectivity Between the RAPID and OSNAP Lines With a Model-Based Data Set. Geophysical Research Letters 50(19):e2023GL105225. https://doi.org/10.1029/2023GL105225

Hátún H, Sandø AB, Drange H, et al (2005) Influence of the Atlantic Subpolar Gyre on the Thermohaline Circulation. Science 309:1841–1844. https://doi.org/10.1126/science.1114777

Hogg NG (1992) On the transport of the Gulf Stream between Cape Hatteras and the Grand Banks. Deep Sea Research Part A Oceanographic Research Papers 39(7-8):1231–1246. https://doi.org/10.1016/0198-0149(92)90066-3

Hunke E, Lipscomb W, Jones P, et al (2017) CICE, The Los Alamos Sea Ice Model. https://doi.org/https://doi.org/10.11578/dc.20171025.1964

Hurrell JW, Deser C (2010) North Atlantic climate variability: The role of the North Atlantic Oscillation . Journal of Marine Systems 79:231–244. https://doi.org/10.1016/j.jmarsys.2009.11.002

Johnson HL, Marshall DP (2002) A Theory for the Surface Atlantic Response to Thermohaline Variability. Journal of Physical Oceanography 32:1121–1132. https://doi.org/10.1175/1520-0485(2002)032⟨1121:ATFTSA⟩2.0.CO;2

Jones BT, Solow A, Ji R (2016) Resource Allocation for Lagrangian Tracking. Journal of Atmospheric and Oceanic Technology 33(6):1225–1235. https://doi.org/10.1175/JTECH-D-15-0115.1

Koman G, Bower AS, Holliday NP, et al (2024) Observed decrease in Deep Western Boundary Current transport in subpolar North Atlantic. Nature Geoscience 17(11):1148–1153. https://doi.org/10.1038/s41561-024-01555-6

Kostov Y, Johnson HL, Marshall DP, et al (2021) Distinct sources of interannual subtropical and subpolar Atlantic overturning variability. Nature Geoscience 14:491–495. https://doi.org/10.1038/s41561-021-00759-4

Kwon YO, Riser SC (2005) General circulation of the western subtropical North Atlantic observed using profiling floats. Journal of Geophysical Research 110(C10):C10012. https://doi.org/10.1029/2005JC002909

Lohmann K, Drange H, Bentsen M (2009) Response of the North Atlantic subpolar gyre to persistent North Atlantic oscillation like forcing. Climate Dynamics 32(2-3):273–285. https://doi.org/10.1007/s00382-008-0467-6

Madec G, Bourdallé-Badie R, Bell M, et al (2019) NEMO ocean engine. Tech. rep., Institut Pierre-Simon Laplace (IPSL), https://doi.org/10.5281/zenodo.1464816

Marsh R, Dey D, Lenn YD, et al (2024) Shifts from surface density compensation to projected warming, freshening and stronger stratification in the subpolar North Atlantic. Climate Dynamics 62(8):8227–8253. https://doi.org/10.1007/s00382-024-07336-6

Marshall DP, Johnson HL (2013) Propagation of Meridional Circulation Anomalies along Western and Eastern Boundaries. Journal of Physical Oceanography 43(12):2699–2717. https://doi.org/10.1175/JPO-D-13-0134.1

Megann A, Blaker A, Coward A, et al (2022) Model output from 1/12° global JRA55-forced integration of GO8p7 global ocean-sea ice model from 1958 to 2021. Tech. rep., NERC EDS British Oceanographic Data Centre NOC, https://doi.org/10.5285/399b0f762a004657a411a9ea7203493a

Meinen CS, Johns WE, Moat BI, et al (2019) Structure and Variability of the Antilles Current at 26.5°N. Journal of Geophysical Research: Oceans 124(6):3700–3723. https://doi.org/10.1029/2018JC014836

Pérez-Hernández MD, Hernández-Guerra A, Cana-Cascallar L, et al (2023) The Seasonal Cycle of the Eastern Boundary Currents of the North Atlantic Subtropical Gyre. Journal of Geophysical Research: Oceans 128(4):e2022JC019487. https://doi.org/10.1029/2022JC019487

Petit T, Robson J, Ferreira D, et al (2025) Coherence of the AMOC Over the Subpolar North Atlantic on Interannual to Multiannual Time Scales. Geophysical Research Letters 52(9):e2025GL115171. https://doi.org/10.1029/2025GL115171

Rio MH, Hernandez F (2003) High-frequency response of wind-driven currents measured by drifting buoys and altimetry over the world ocean. Journal of Geophysical Research 108(C8):3283. https://doi.org/10.1029/2002JC001655

Robson J, Polo I, Hodson DLR, et al (2018) Decadal prediction of the North Atlantic subpolar gyre in the HiGEM high-resolution climate model. Climate Dynamics 50(3-4):921–937. https://doi.org/10.1007/s00382-017-3649-2

Roessler A, Rhein M, Kieke D, et al (2015) Long-term observations of North Atlantic Current transport at the gateway between western and eastern Atlantic. Journal of Geophysical Research: Oceans

120(6):4003–4027. https://doi.org/10.1002/2014JC010662

Rypina II, Pratt LJ, Lozier MS (2011) Near-Surface Transport Pathways in the North Atlantic Ocean: Looking for Throughput from the Subtropical to the Subpolar Gyre. Journal of Physical Oceanography 41:911–925. https://doi.org/10.1175/2011JPO4498.1

Sanders RNC, Jones DC, Josey SA, et al (2022) Causes of the 2015 North Atlantic cold anomaly in a global state estimate. Ocean Science 18(4):953–978. https://doi.org/10.5194/os-18-953-2022

Smeed DA, Johns WE, Smith RH, et al (2026) Overturning Circulation of the North Atlantic Subtropical Gyre Computed in Density Coordinates at 26°N. Geophysical Research Letters 53(5). https://doi.org/10.1029/2025GL118277

Stevens SW, Johnson RJ, Maze G, et al (2020) A recent decline in North Atlantic subtropical mode water formation. Nature Climate Change 10:335–341. https://doi.org/10.1038/s41558-020-0722-3

Sutton RT, Dong B (2012) Atlantic Ocean influence on a shift in European climate in the 1990s. Nature Geoscience 5(11):788–792. https://doi.org/10.1038/ngeo1595

Tooth OJ, Foukal NP, Johns WE, et al (2024) Lagrangian Decomposition of the Atlantic Ocean Heat Transport at 26.5°N. Geophysical Research Letters 51(14). https://doi.org/10.1029/2023GL107399

Tooth OJ, Johnson HL, Wilson C (2025) Controls on dense-water formation along the path of the North Atlantic subpolar gyre. Ocean Science 21(5):2101–2123. https://doi.org/10.5194/os-21-2101-2025

Tsujino H, Urakawa S, Nakano H, et al (2018) JRA-55 based surface dataset for driving ocean–sea-ice models (JRA55-do). Ocean Modelling 130:79–139. https://doi.org/10.1016/j.ocemod.2018.07.002

Wanner H, Brönnimann S, Casty C, et al (2001) North Atlantic Oscillation - Concepts and Studies. Surveys in Geophysics 22:321–382. https://doi.org/https://doi.org/10.1023/A:1014217317898

Zhang R (2010) Latitudinal dependence of Atlantic meridional overturning circulation (AMOC) variations. Geophysical Research Letters 37(16):L16703. https://doi.org/10.1029/2010GL044474

Supplementary Files

This is a list of supplementary files associated with this preprint. Click to download.

- SupplementarythroughputofGSwater190526.pdf